FIGURE 7. Mean flow rate (A) and regurgitation rate (B) at every 10 bpm from 70 to 120 bpm.

robust because the tissues were originally formed as a conduit. The burst strength of the leaflets of the stent-biovalve was over 7600 mmHg, which was about 2 times larger than that of canine pulmonary valve leaflets (3600 ± 780 mmHg) and over that of aortic valve leaflets (6200 ± 1400 mmHg).[16] In addition, elastic modulus of the leaflets of the stent-biovalve was 2.6 ± 1.1 MPa, which was over 2 times larger than that of goat aortic valve leaflets (1.1 ± 0.4 MPa). The cells in the leaflet tissue of the stent-biovalve were rare as shown in Figure 5. Therefore, it was considered that there was little influence of cells in the biomechanics. The connective strength between biovalve leaflet and stent was comparable to native aortic valve and conduit. Therefore, we believe strongly that the robust properties of valve leaflets of the stent-biovalve were demonstrated by these mechanical results.

To facilitate the use of the stent-biovalve in TAVI, a self-expandable nitinol stent was chosen in this study, which is typically used for TAVI (CoreValve, Medtronic, MN). For transcatheter implantation, the CoreValve is crimped into a sheathed catheter under low temperature conditions.[18] The valve leaflet for TAVI thus requires adequate durability and a strong tissue connection with the stent for successful crimping into the sheathed catheter. The stent-biovalves constructed in this study showed favorable valve function even after eversion (inside out) under low temperature conditions (iced water). This handling exposed the valve leaflets to conditions that were more severe than crimping. Even after turning the stent inside out, the valve leaflets remained strongly connected with the stent [Figure 1(D)], which did not tear apart even by pulling with forceps, as demonstrated in the type IV biovalve, which was strongly attached to a scaffold material.[14] Therefore, it is highly expected that the valve leaflets of the stent-biovalve would have sufficient durability and a robust tissue connection with the stent for crimping into a sheathed catheter for TAVI.

Because the biovalve is an engineered tissue, it will have to maintain its function in living bodies, and the living body would be the best environment for testing the biovalve. Therefore, we believe that there is little value in examining the long-term durability of the biovalve in an in vitro system. However, in separate study, we evaluated the durability of the biovalve in in-vitro pulsatile flow of saline.[19] Even after biovalve pulsated more than four million times (heart rate = 70 bpm; mean flow rate = 5.0 L/min; mean aortic pressure = 92 mm Hg), stable continuous operation was possible without excessive reduction of the flow rate or bursting. However, in our recent report, postoperative echocardiography showed smooth movement of the leaflets of the biovalve with little regurgitation under systemic circulation (2.6 ± 1.1 L/min) at least for 2 months of implantation to goat in an apico-aortic bypass model.[17] Therefore, we believe that the stent-biovalve has similar excellent durability in in vitro and in vivo.

Recently, several studies reported that tissue engineered valved stents were successfully implanted as pulmonic valve in vivo.[20–23] These materials may overcome the limitations of bioprosthetic heart valve prostheses and may be expected further evolution to be applied to clinical use. However, these tissue-engineered valved stents require complicated cell management protocols with cell culture under strictly sterile conditions, and also require decellularized allografts or synthetic scaffold materials to seed autologous cells. In this study, autologous heart valve with stent (stent-biovalve) showed favorable valve function, without expensive facilities or complicated manipulations. Stent-biovalve may overcome the limitations of bioprosthetic heart valve prostheses and have the advantage of other tissue engineered valved stents.

In this study, the pulsatile circuit was designed for actual human aortic valve conditions (mean flow = 5 L/min; mean pressure = 100 mmHg; heart rate = 70–100 bpm); however, saline solution was selected as a working fluid. The kinetic viscosity of blood is 4.4×10^{-6} m^2/s, which is

~4 times that of saline solution (1.0×10^{-6} m^2/s). Thus, our circuit did not approximate the viscosity of blood; however, it was considered that the present design achieved an adequate performance of valvular function for a future animal implantation study. We do not have any additional data on the biomechanics of the tissue affected after long-term stress. However, this is our near future research topics. We are now planning implantation study of the stent-biovalve to beagle dogs. However, we previously reported that in the tissue of the biotube, which was also obtained by IBTA technology from rod molds, the elastic modulus value of the biotube after implantation was 2× higher than that of the native arteries. The biotube after implantation acquired further robust property of maintenance of the preimplantation elongation ability.

Based on the American College of Cardiology/American Heart Association valvular guidelines 2006,[2] the regurgitant fraction of the present stent-biovalve was much lower than the "mild" classification, in fact being present at "trace" levels. Yare et al. reported that 75% of bioprosthetic valves used for TAVI showed trace to mild aortic regurgitation (AR) after implantation; however, such AR did not affect LV structure and function.[24] Previous biovalves were demonstrated to have favorable valve function and histological changes when used as heart valves in a beagle model[14]; further, biotubes created by IBTA technology regenerated arteries within 3 months of implantation.[25] Therefore, although this evaluation of the stent-biovalve was performed *in vitro*, it is expected that this stent-biovalve with autologous valve leaflets will show more favorable function *in vivo* than *in vitro*. We expect that this stent-biovalve could eventually be applied for TAVI, with favorable valve function *in vivo*.

CONCLUSION

We successfully developed a novel method for efficient construction of a robust, completely autologous heart valve eversion of a self-expandable stent, and named the resulting product the stent-biovalve. These stent-biovalves were obtained after only 4 weeks of subcutaneous embedding in a beagle dog or a goat. Owing to the large and robust leaflet tissues that were developed in the open-form position, excellent in vitro valve function was achieved. Future studies are expected to focus on the implantation of this stent-biovalve in animal models to confirm chronic valve function and durability in vivo.

REFERENCES

1. Iung B, Baron G, Butchart EG, Delahaye F, Gohlke-Bärwolf C, Levang OW, Tornos P, Vanoverschelde JL, Vermeer F, Boersma E, Ravaud P, Vahanian A. A prospective survey of patients with valvular heart disease in Europe: The Euro Heart Survey on Valvular Heart Disease. Eur Heart J 2003;24:1231–1243.
2. Bonow RO, Carabello BA, Chatterjee K, de Leon AC Jr, Faxon DP, Freed MD, Gaasch WH, Lytle BW, Nishimura RA, O'Gara PT, O'Rourke RA, Otto CM, Shah PM, Shanewise JS, Smith SC Jr, Jacobs AK, Adams CD, Anderson JL, Antman EM, Fuster V, Halperin JL, Hiratzka LF, Hunt SA, Lytle BW, Nishimura R, Page RL, Riegel B. ACC/AHA 2006 guidelines for the management of patients with valvular heart disease: A report of the American College of Cardiology/American Heart Association Task Force on Practice Guidelines (writing committee to revise the 1998 Guidelines for the Management of Patients With Valvular Heart Disease). J Am Coll Cardiol 2006;48:e1–148.
3. Iivanainen AM, Lindroos M, Tilvis R, Heikkilä J, Kupari M. Natural history of aortic valve stenosis of varying severity in the elderly. Am J Cardiol 1996;78:97–101.
4. Le Tourneau T, Savoye C, McFadden EP, Grandmougin D, Carton HF, Hennequin JL, Dubar A, Fayad G, Warembourg H. Mid-term comparative follow-up after aortic valve replacement with Carpentier-Edwards and Pericarbon pericardial prostheses. Circulation 1999;100(19 Suppl):II11–16.
5. Cribier A, Eltchaninoff H, Bash A, Borenstein N, Tron C, Bauer F, Derumeaux G, Anselme F, Laborde F, Leon MB. Percutaneous transcatheter implantation of an aortic valve prosthesis for calcific aortic stenosis: First human case description. Circulation 2002; 106:3006–3008.
6. Latib A, Maisano F, Bertoldi L, Giacomini A, Shannon J, Cioni M, Ielasi A, Figini F, Tagaki K, Franco A, Covello RD, Grimaldi A, Spagnolo P, Buchannan GL, Carlino M, Chieffo A, Montorfano M, Alfieri O, Colombo A. Transcatheter vs surgical aortic valve replacement in intermediate-surgical-risk patients with aortic stenosis: A propensity score-matched case-control study. Am Heart J 2012;164:910–917.
7. Bloomfield P, Wheatley DJ, Prescott RJ, Miller HC. Twelve-year comparison of a Bjork-Shiley mechanical heart valve with porcine bioprostheses. N Engl J Med 1991;324:573–579.
8. Hammermeister K, Sethi GK, Henderson WG, Grover FL, Oprian C, Rahimtoola SH. Outcomes 15 years after valve replacement with a mechanical versus a bioprosthetic valve: Final report of the Veterans Affairs randomized trial. J Am Coll Cardiol 2000;36:1152–1158.
9. Emmert MY, Weber B, Wolint P, Behr L, Sammut S, Frauenfelder T, Frese L, Scherman J, Brokopp CE, Templin C, Grünenfelder J, Zünd G, Falk V, Hoerstrup SP. Stem cell-based transcatheter aortic valve implantation: First experiences in a pre-clinical model. JACC Cardiovasc Interv 2012;5:874–883.
10. Metzner A, Stock UA, Iino K, Fischer G, Huemme T, Boldt J, Braesen JH, Bein B, Renner J, Cremer J, Lutter G. Percutaneous pulmonary valve replacement: Autologous tissue-engineered valved stents. Cardiovasc Res 2010;88:453–461.
11. Nakayama Y, Ishibashi-Ueda H, Takamizawa K. In vivo tissue-engineered small-caliber arterial graft prosthesis consisting of autologous tissue (biotube). Cell Transplant 2004;13:439–449.
12. Hayashida K, Kanda K, Yaku H, Ando J, Nakayama Y. Development of an in vivo tissue-engineered, autologous heart valve (the biovalve): Preparation of a prototype model. J Thorac Cardiovasc Surg 2007;134:152–159.
13. Hayashida K, Kanda K, Oie T, Okamoto Y, Ishibashi-Ueda H, Onoyama M, Tajikawa T, Ohba K, Yaku H, Nakayama Y. Architecture of an in vivo-tissue engineered autologous conduit "Biovalve". J Biomed Mater Res B Appl Biomater 2008;86:1–8.
14. Yamanami M, Yahata Y, Tajikawa T, Ohba K, Watanabe T, Kanda K, Yaku H, Nakayama Y. Preparation of in-vivo tissue-engineered valved conduit with the sinus of Valsalva (type IV biovalve). J Artif Organs 2010;13:106–112.
15. Nakayama Y, Yahata Y, Yamanami M, Tajikawa T, Ohba K, Kanda K, Yaku H. A completely autologous valved conduit prepared in the open form of trileaflets (type VI biovalve): mold design and valve function in vitro. J Biomed Mater Res B Appl Biomater 2011;99:135–141.
16. Yamanami M, Yahata Y, Uechi M, Fujiwara M, Ishibashi-Ueda H, Kanda K, Watanabe T, Tajikawa T, Ohba K, Yaku H, Nakayama Y. Development of a completely autologous valved conduit with the sinus of Valsalva using in-body tissue architecture technology: A pilot study in pulmonary valve replacement in a beagle model. Circulation 2010;122 (11 Suppl):S100–106.
17. Takewa Y, Yamanami M, Kishimoto Y, Arakawa M, Kanda K, Matsui Y, Oie T, Ishibashi-Ueda H, Tajikawa T, Ohba K, Yaku H, Taenaka Y, Tatsumi E, Nakayama Y. In vivo evaluation of an in-body, tissue-engineered, completely autologous valved conduit (biovalve type VI) as an aortic valve in a goat model. J Artif Organs 2012;16:176–184.

279

18. Grube E, Laborde JC, Gerckens U, Felderhoff T, Sauren B, Buellesfeld L, Mueller R, Menichelli M, Schmidt T, Zickmann B, Iversen S, Stone GW. Percutaneous implantation of the CoreValve self-expanding valve prosthesis in high-risk patients with aortic valve disease: The Siegburg first-in-man study. Circulation 2006; 114:1616–1624.

19. Sumikura H, Nakayama Y, Ohnuma K, Takewa Y, Tatsumi Y. In vitro evaluation of a novel autologous aortic valve (Biovalve) with a pulsatile circulation circuit. Artif Organs. Forthcoming.

20. Weber B, Scherman J, Emmert MY, Gruenenfelder J, Verbeek R, Bracher M, Black M, Kortsmit J, Franz T, Schoenauer R, Baumgartner L, Brokopp C, Agarkova I, Wolint P, Zund G, Falk V, Zilla P, Hoerstrup SP. Injectable living marrow stromal cell-based autologous tissue engineered heart valves: First experiences with a one-step intervention in primates. Eur Heart J 2011;32:2830–2840.

21. Schmidt D, Dijkman PE, Driessen-Mol A, Stenger R, Mariani C, Puolakka A, Rissanen M, Deichmann T, Odermatt B, Weber B, Emmert MY, Zund G, Baaijens FP, Hoerstrup SP. Minimally-inva-sive implantation of living tissue engineered heart valves: A com-prehensive approach from autologous vascular cells to stem cells. J Am Coll Cardiol. 2010;56:510–520.

22. Metzner A, Stock UA, Iino K, Fischer G, Huemme T, Boldt J, Braesen JH, Bein B, Renner J, Cremer J, Lutter G. Percutaneous pulmonary valve replacement: autologous tissue-engineered valved stents. Cardiovasc Res 2010;88:453–461.

23. Lutter G, Metzner A, Jahnke T, Bombien R, Boldt J, Iino K, Cremer J, Stock UA. Percutaneous tissue-engineered pulmonary valved stent implantation. Ann Thorac Surg 2010;89:259–263.

24. Yared K, Garcia-Camarero T, Fernandez-Friera L, Llano M, Durst R, Reddy AA, O'Neill WW, Picard MH. Impact of aortic regurgita-tion after transcatheter aortic valve implantation: Results from the REVIVAL trial. JACC Cardiovasc Imaging 2012;5:469–477.

25. Watanabe T, Huang H, Hayashida K, Okamoto Y, Nemoto Y, Kanda K, Yaku H, Nakayama Y. Development of small-caliber "Biotube" vascular grafts: Preliminary animal implantation study. Artif Organs 2005;29:733.

Treatment of rabbit carotid aneurysms by hybrid stents (microporous thin polyurethane-covered stents): Preservation of side-branches

Shogo Nishi[1], Yasuhide Nakayama[2], Hatsue Ishibashi-Ueda[3], Masato Yoshida[4] and Hiroshi Yonetani[1]

Abstract

Objective: We sought to determine the patency of normal arterial branches from the covered segments of an artery after stenting.

Background: Most intracranial aneurysms occur at arterial branching points (bifurcations, side-branches, or perforators). The post-stenting patency of normal arterial branches from the covered segments of the artery is important. We have previously developed a hybrid stent with micropores to prevent early parent artery occlusion by more early endothelialization, and mid- to long-term parent artery stenosis by control of intimal hyperplasia after aneurysm occlusion.

Methods: We created aneurysms in 10 rabbits by distal ligation and intraluminal incubation of elastase within an endovascularly trapped proximal segment of the common carotid artery. All animals were treated with hybrid stents having micropores. Four animals were observed for one month and three each for three and 12 months. The patency of the side-branches of the subclavian artery was evaluated angiographically and in some cases, histologically.

Results: Aneurysms were completely occluded at all time points other than 12 months. The subclavian artery and brachiocephalic artery were patent, without significant stenosis. All the side-branches of the subclavian artery detected on the preoperative angiogram remained patent at the final assessment.

Conclusion: The use of hybrid stents for aneurysm repair and side-branch patency seems to be effective, as per the long-term results obtained in an animal model.

Keywords

Aneurysm, intravascular stent, polyurethane, porosity, endothelium, intimal hyperplasia

Introduction

Most intracranial aneurysms occur at arterial branching points (bifurcations, side-branches, or perforators). Simple covered stents are associated with the highest rate of complete aneurysm occlusion. However, their use in the human intracranial circulation is limited by access issues and the possibility of occluding small perforating end-arteries. It is important to assess the patency of normal arterial branches arising from the covered segments of the artery after implantation of simple covered stents. We established rabbit carotid aneurysms by intraluminal incubation of elastase within an endovascularly trapped segment of the proximal common carotid artery (CCA),[1,2] and we implanted hybrid stents equipped with micropores in these

aneurysms.[3] Besides studying the occlusive effect of the hybrid stents in the aneurysms, we examined the patency

[1]Department of Neurosurgery, Neuro-Intervention, Spinal Surgery, Sapporo-Higashi Tokushukai Hospital, Sapporo, Hokkaido, Japan
[2]Division of Medical Engineering and Materials, National Cerebral and Cardiovascular Center Research Institute, Suita, Osaka, Japan
[3]Department of Pathology, National Cerebral and Cardiovascular Center Hospital, Suita, Osaka, Japan
[4]Department of Neurosurgery, Nozaki Tokushukai Hospital, Nozaki, Osaka, Japan

Corresponding author:
Shogo Nishi, Department of Neurosurgery, Neuro-Intervention, Spinal Surgery, Sapporo Higashi-Tokushukai Hospital, 14-3-1, Higashi, N33, Higashi-ku, Sapporo, Hokkaido 065-0033, Japan.
Email: nishi@higashi-tokushukai.or.jp

of the side-branches arising from the right subclavian artery (SA), both angiographically and histologically.

Materials and methods

All experiments were performed on Japanese white rabbits (3.5–4.2 kg) and conducted in accordance with the Principles of Laboratory Animal Care (formulated by the National Society for Medical Research, Chicago, IL) and the Guide for the Care and Use of Laboratory Animals (NIH publication no. 86–23, revised 1985; National Institute of Health, Bethesda, MD). The research protocol (no. 12010) was approved by the ethics committee of the National Cerebral and Cardiovascular Center Research Institute.

The aneurysms were first created and then subjected to stent implantation two to four weeks later under general anesthesia, which was induced by the intramuscular injection of 0.2 ml/kg ketamine chloride (10%) and 0.3 ml/kg xylazine, and additional dosage was determined on the basis of the animal's movements.

Fabrication of hybrid stents (Figure 1)

A stainless mold (diameter, 1 mm) was dipped in a tetrahydrofuran solution and allowed to dry. Subsequently, a balloon-expandable coronary-artery bare stent (Momo stent: diameter, 3 mm; length, 20 mm; Japan Stent Technology, Okayama, Japan) was mounted on the cover film of the mold, and again, it was dipped in the solution and dried. The thickness of the cover film was restricted to approximately 30 μm. Micropores were then made in the cover film using a KrF excimer laser apparatus (L4500; Hamamatsu Photonics, Shizuoka, Japan). Micropores are circular, with a pore diameter and interpore distance of 100 μm and 250 μm, respectively, such that they achieve an opening ratio of 23.6% (calculated) after full expansion.[3] The uncoated stent was a bare

stent with an opening ratio of 86%. The outer surface of the film of the microporous stent grafts was coated with argatroban (500 μg/cm^2), which was applied using a methanol solution (1% w/v); the solvent was subsequently volatilized for physical adsorption. The fabricated hybrid stent was then remounted on the delivery balloon system (Thrill Slalom PTA dilatation balloon catheter; diameter, 3 mm; length, 2 cm; Cordis, J & J, Europa, N. V., Netherlands).

Preparation of aneurysms in rabbits (Figure 2(a))

Aneurysms were constructed in 10 female rabbits by employing a previously described method,[1,2] with a few simple modifications. The right CCA was surgically isolated, ligated distally, and controlled proximally with 2.0 silk sutures before a 5-Fr detachable sheath introducer (Medikit, Tokyo, Japan) was induced and passed retrograde to the midportion of the CCA (approximately 3 cm cephalad to the origin of the CCA). A hemostatic valve of the sheath (Medikit, Tokyo, Japan) was detached, and a rotational and hemostatic triple connecter was connected to the sheath placed in the CCA. Through the sheath, an occlusive microballoon (Naviballoon; Kaneka, Tokyo, Japan) (Titan percutaneous transluminal coronal angioplasty (PTCA) dilatation balloon catheter: diameter, 4.0 mm; length, 9 mm; Cordis, J & J, Miami, Florida, USA) and subsequently a microcatheter (Excelsior SL10; Striker, Tokyo, Japan) were advanced near the CCA origin (Figure 2(b)). Porcine elastase (Sigma, Tokyo, Japan) was mixed with nonionic contrast medium to obtain a 25% dilution. Elastase (6.8 units/mg/0.25 cc) was injected and incubated in the isolated CCA for 20 min, while the balloon was inflated at the origin of the right CCA. Next, the microcatheter and deflated microballoon were removed. Angiography was performed to confirm the dilation of the affected CCA. The CCA was ligated with
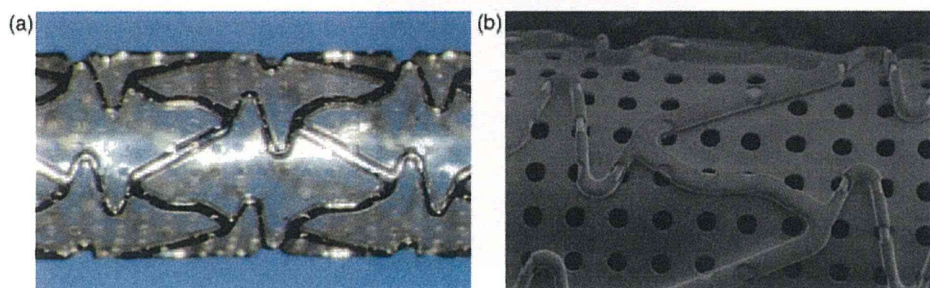

Figure 1. A hybrid stent is shown. Micropores (with a pore diameter and interpore distance of 100 μm and 250 μm, respectively, to accomplish an opening ratio of 23.6% after full expansion) are placed in a polyurethane membrane of approximately 30-μm thickness on a bare coronary stent (a coronary Momo stent, Japan Stent Technology). (a) Macroscopic image and (b) scanning electron microscopic image.

a 2.0 silk thread after sheath removal, and the skin was closed by discontinuous knots with a similar thread.

Endovascular technique

No drugs, such as antiplatelets, were administered during the study. Endovascular treatment was performed via the right femoral artery, at two to four weeks after the creation of the aneurysm. The femoral artery was exposed and ligated distally with a 2.0 silk thread. After pharmacological dilation of the artery with 8 mg of papaverine chloride, a 19-G puncture needle was used to introduce the 0.032″ mandrel; then, a 4-Fr 10-cm sheath (Clinical Supply, Tokyo, Japan) was advanced into the right femoral artery under fluoroscopic guidance.

The 4-Fr catheter was navigated into the brachiocephalic artery (BCA) with a 0.035″ guidewire. Digital subtraction angiography (DSA) showed the BCA, SA, and aneurysm. A balloon catheter (Thrill Slalom PTA dilatation balloon catheter; diameter, 3 mm; length, 2 cm; Cordis, J & J, Europa, N.V., Netherlands) crimped with our hybrid stent was passed through the sheath and navigated into the BCA. Using fluoroscopy and road

mapping, we advanced the hybrid stent over the balloon catheter across the aneurysmal neck and inflated the balloon. Post-procedural DSA was performed. The balloon catheter was removed, leaving the hybrid stent in place. Subsequently, the sheath introducer was carefully and slowly pulled out. The femoral artery was ligated with two sutures of a 2.0 silk thread previously placed around the artery, and the skin was closed discontinuously with a similar thread.

Final angiography and harvesting

After the observation period, angiography was performed using a 4-Fr sheath placed at the left CCA in all animals. The left CCA was exposed and ligated distally. A 19-G puncture needle was used to introduce the 0.032″ mandrel; then, a 4-Fr, 10-cm long sheath (Clinical Supply, Tokyo, Japan) was advanced to the left proximal CCA under fluoroscopic guidance. A DSA series was performed to evaluate the final angiographic result. Occlusion of the aneurysms and patency of preoperatively detected side-branches of the artery was evaluated angiographically. Thereafter, the animals were subjected to euthanasia by
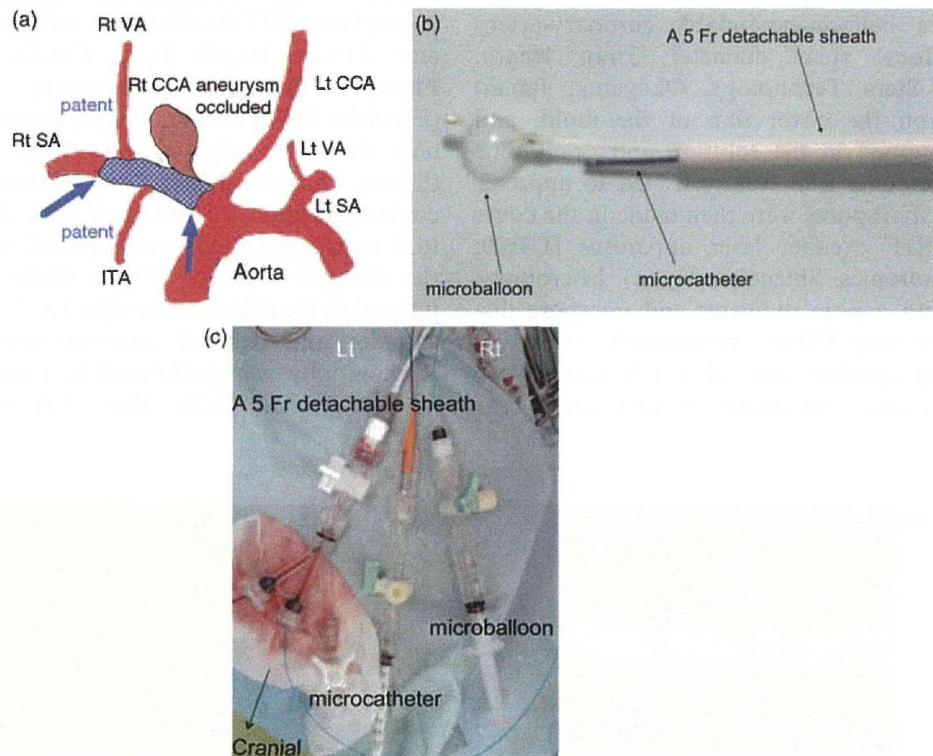

Figure 2. A schema of the aneurysm occlusion in the rabbit using a hybrid stent (arrows) implanted through the femoral artery. Branches such as the vertebral artery, internal thoracic artery, and costocervical artery are indicated (a). Approach to the right CCA via a rotational and hemostatic triple connector. A microcatheter and microballoon are inserted from each hemostatic valve (b). Entrapment system in the right CCA. A microballoon and microcatheter through a 5-Fr detachable sheath (c). CCA: common carotid artery; VA: vertebral artery; ITA: internal thoracic artery; SA: subclavian artery.

intravenous injection of potassium chloride. The BCA, the right SA, vertebral artery (VA), some other arterial branches, and the treated aneurysm were resected en bloc and placed directly in a 4% paraformaldehyde phosphate-buffered saline solution for rapid fixation. Some of the samples were evaluated histologically to determine the patency of the branches.

Histology

Histological examination was performed in some cases, by using a cross-sectional sample (hematoxylin and eosin (H&E) stain) obtained from the stented portion of the aneurysm to confirm the patency of the side-branches.

Results

A balloon catheter crimped with our hybrid stent was easily and smoothly passed through the sheath, navigated into the BCA and right SA via the aorta, and inflated at the neck of the aneurysm. The hybrid stent covered and occluded the aneurysm instantly or after a few minutes. All the side-branches of the right SA observed preoperatively appeared patent (without any significant stenosis) on the angiograms obtained at one, six, and 12 months.

Stent graft and its remounting

The stent struts were completely embedded within the cover film, thereby indicating that the luminal surface of the stent graft was smooth and flat (Figure 1(a) and (b)). It was possible to shrink the stent grafts by using a hand-held crimping device, without any damage to the cover film. Stenting procedures were performed using standard endoscopic procedures without difficulty.[3,4]

Fabrication of carotid aneurysms (Figure 2(c))

All aneurysms were systematically and easily created by our modified method. A 5-Fr detachable sheath introducer, later connected with a rotational and hemostatic triple connector, was easily inserted into the affected CCA. An occlusive balloon and microcatheter were navigated into the CCA origin without difficulty. The size and shape of the aneurysms were variable, although they were originally funnel-shaped.

Occlusion of the aneurysm (Table 1)

At 12 months, all aneurysms but one were completely occluded, with four aneurysms being occluded at one month; three, at three months (Figure 3(a) and (b));

Table 1. Results.

Months	Numbers	Aneurysm Occlusion	Branches Patency
1	4	4	All[a]
3	3	3	All[a]
12	3	2[b]	All[a]

All aneurysms but one were occluded at 12 months: four aneurysms at one month; three at three months; and two at 12 months. At 12 months, one aneurysm was patent because of distal movement of the stent graft itself from the aneurysm neck at the initial stent placement. Side-branches were the right vertebral artery, internal thoracic artery, costocervical artery, and other small branches. All side-branches drawn preoperatively on the angiogram were visible after occlusion and before the rabbits were euthanized.
[a]Vertebral artery, internal thoracic artery, costocervical artery, etc.
[b]Open in one, due to stent migration.

and two, at 12 months (Figure 4(a) and (b)). At the 12-month follow-up, one aneurysm remained patent because of distal movement of the hybrid stent itself from the aneurysm neck.

Preservation of side-branches

The side-branches were the right VA, internal thoracic artery, costocervical artery, and other small branches. All the side-branches detected on the angiogram before the operation were visible after the occlusion and before the rabbits were killed (Table 1; Figures 3(a,b) and 4(a,b)). H&E staining revealed that the orifice of the branch from the right SA was patent (Figure 4(c)).

Discussion

Although Guglielmi detachable coil systems (GDC coils) have been widely accepted and used in the treatment of intracranial aneurysms, primary stenting of aneurysms by using porous stents[5] or stent grafts[6] and implantation of coils after stenting[7–10] are emerging techniques in endovascular treatment.

The development of stent grafts for intracranial aneurysms is challenging. Most intracranial aneurysms occur at branch points (bifurcation, small side-branches, and perforating arteries). The maintenance of the patency of normal arterial branches originating from the covered segment of the artery after stenting across the lesion is a major concern. The salient issues influencing the use of stent grafting for aneurysms in humans include the delivery of the stent graft, degree of cover porosity, configuration of the aneurysm, curvature of the parent vessel, and presence or absence of perforating end-arteries.[2]

A simple bare stent has no efficacious occlusive effect on aneurysms, although it raises a few concerns about
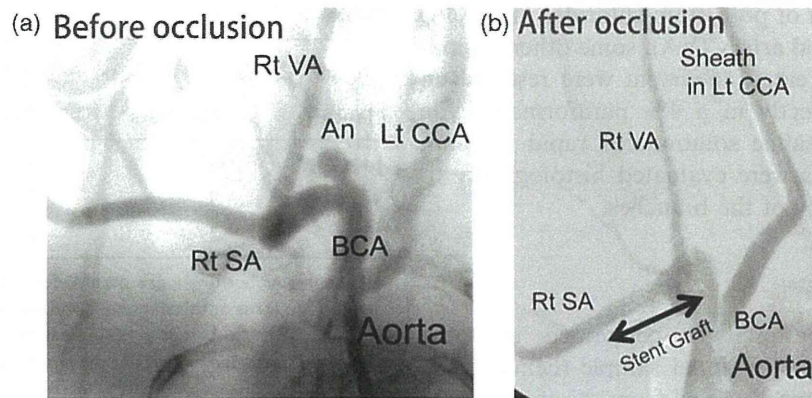
Figure 3. At three months after occlusion, the aneurysm was still occluded (before (a) and after (b)). Side-branches, such as the vertebral artery and costocervical artery, were patent. An arrow shows a stent graft placed a cross the aneurysmal neck (b). CCA: common carotid artery; VA: vertebral artery; BCA: brachiocephalic artery; SA: subclavian artery.
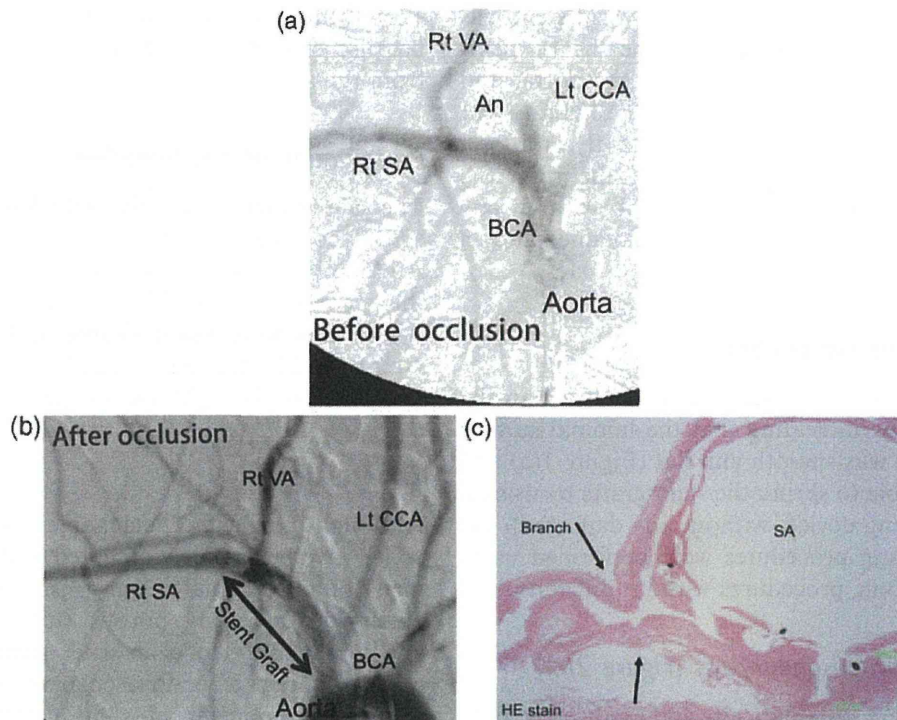

Figure 4. At 12 months after occlusion, the aneurysm was completely occluded (pre (a) and post (b)), while the vertebral artery, internal thoracic artery, and costocervical artery remained patent. An arrow shows a stent graft placed across the aneurysmal neck (b). A cross-sectional specimen (H&E stain) showed that the origin of the branch (arrows) from the subclavian artery was patent at 12 months (c). CCA: common carotid artery; VA: vertebral artery; BCA: brachiocephalic artery; SA: subclavian artery; H&E stain: hematoxylin and eosin stain.

the occlusion of side-branches. In contrast, a simple covered stent has sufficient occlusive effect on the aneurysms, but it can occlude the side-branches. To compensate for the disadvantages of simple covered stents, we have been developing a hybrid stent. This hybrid stent consists of the commercially available balloon-expandable coronary-artery stent with a thin SPU film (by dip-coating method) on which micropores have been created by the excimer laser ablation technique, followed by coating with argatroban.[4] We have developed a hybrid stent with micropores to prevent early parent artery occlusion by more early endothelialization and administration of argatroban, and mid- to long-term parent artery stenosis by control of intimal

hyperplasia after aneurysm occlusion, compared with those in a simple covered stent.

In the current study, we established elastase-induced rabbit carotid aneurysms, all of which were occluded by our hybrid stents until 12 months, and all the small side-branches detected preoperatively remained patent without significant stenosis or occlusion even after implantation of the hybrid stents. The hybrid stent was smoothly navigated into the affected BCA and SA from the femoral artery, as easily as the bare stents.

Our microporous membrane induces early endothelialization capable of secreting tissue plasminogen[11] within one week of stent graft implantation,[3] thereby avoiding early thrombosis and controlling mid- to long-term hyperplasia.[12] Polyurethane has excellent elastomeric properties and is clinically used as a material for manufacturing blood pumps and arterial grafts; it also exhibits no toxicity or little biodegradation.[13–15] Argatroban, an arginine-derived synthetic low-molecular-weight compound that binds to thrombin, competitively inhibits fibrinogen cleavage and the platelet activation stimulated by thrombin.[16,17] It has been used for preparing antithrombogenic surfaces in percutaneous transluminal angioplasty (PTA) devices, including balloon catheters and stents.[18,19]

In this study, cerebral thromboembolic events were not evaluated using magnetic resonance imaging (MRI). Less intimal hyperplasia of the parent artery was focally noted in the group treated with hybrid stents without antiplatelets. If this device is clinically used, antiplatelet therapy with one or two drugs will be necessary for approximately one to three months, as per the conventional therapy after vascular stenting.

The aneurysms were created experimentally by intraluminal incubation of elastase within an endovascularly trapped segment of the proximal portion of the CCA, with slight modifications to the method. The CCA branches from the BCA of the rabbit, and it was ligated beyond the point of elastase incubation. Endoluminal digestion of the internal elastic lamina, with spreading of elastase up to the adventitia, results in a thin-walled aneurysm, as observed in humans.[20] Aneurysm formation occurred over a two-week period, after which the animals were treated with the respective therapies. The rabbit aneurysm model with elastase has some characteristic features: (1) long-term patency in untreated animals, (2) simulating aneurysm morphologies that place a high shear stress on the aneurysmal neck, (3) similar size in aneurysm diameter and parent artery diameter, (4) maintenance of the integrity of the endothelium of the aneurysmal cavity, and (5) short construction time and easy reproduction.[21] The rabbit aneurysm is histologically similar to the human saccular aneurysm and was useful for the current study.

Mechanisms of branch occlusion by stents include the longitudinal snow-plowing effect, stent jailing (early stage), and in-stent neointimal growth (late stage) during or after stent deployment.[22] Cerebral vessels with aneurysms tended to be minimally atherosclerotic. Radial force in the stent strut might be less than that in the intracranial PTA stent, which reduced the longitudinal redistribution of the plaque. Our hybrid stent had a porosity appropriate for the regulation of the in-stent neointima growth even at 12 months (personal communication). The arteriovenous pressure gradient is the driving force of the blood flow through the branches and perforators under normal conditions. Additionally, long-term remodeling of the artery and its lumen, in response to the presence of the intraluminal prosthesis, is less likely to result in complete occlusion of the jailed branch.[22] Experimental evidence in dogs showed that vessels (small muscular branches from the VA) comparable to human perforators tend to remain patent if less than 50% of the ostial diameter is covered with the stent strut.[23] If the diameter of struts is 100 μm, complete occlusion of the perforators may not occur, but the exposed stent wire covering the perforators will remain a potential source of thromboembolic complications in canine carotid aneurysm models.[24] The diameter of stent struts in our hybrid stent was less than 50 μm. Fibrotic tissue growth around the filaments extended into the origin of the branches (external arteries) without narrowing them significantly.

Intracranial self-expanding stents generate a radial force too weak to require coverage with cover materials, although some of them, such as Neuroform or Enterprise, are recommended. Therefore, we selected balloon-expandable coronary-artery stents for the preparation of hybrid stents.

The branch originating from the aneurysm sac, which is treated with a flow diverter (pipeline embolization device), is kept patent in the presence of a flow demand through it.[25] The significant shrinkage of the aneurysm gives the branch an "infundibular-like" appearance at its origin, or the branch is represented by a tortuous takeoff from the parent artery in place of the initial aneurysm. A slow occlusion process for the treatment of ruptured aneurysms is yet to be developed.

The stent developed by us is a hybrid of a bare stent and a simple covered stent; this hybrid nature helps regulate the porosity and enables early intraluminal endothelialization and late inhibition of the intimal hyperplasia. Experimentally fabricated canine carotid aneurysms were occluded with the placement of our hybrid, self-expanding, stent grafts at one,[4] six, and 12 months (personal communication). A porosity of 23.6% was found to be suitable in the presence of less neointimal hyperplasia.[4] On the basis of the porosity and demand of the blood flow by vessels, side-branches

or perforating arteries can be protected if the stenotic area generated by the hybrid stents is less than 50%.[23]

In this study, the patency of all the side-branches was maintained, along with the occlusion of the aneurysms, although the side-branches were not as narrow as the intracranial perforators. If the use of hybrid stents for aneurysmal occlusion is planned, the number of associated perforators should be less to ensure safety.

In the examined aneurysmal model using stent grafts, all small side-branches of the patent artery were patent without significant stenosis. Thus, our hybrid stent represents a step forward in the clinical management of aneurysms.

Conclusion

The long-term results obtained in an animal model indicate that hybrid stents may be effective for aneurysm repair while maintaining side-branch patency.

Acknowledgements

Abbreviations

CCA	Common carotid artery
ICA	Internal carotid artery
BCA	Brachiocephalic artery
SA	Subclavian artery
VA	Vertebral artery
PCoA	Posterior communicating artery
OPhA	Ophthalmic artery
AChA	anterior choroidal artery
PICA	Posterior inferior cerebellar artery
PTCA	Percutaneous transluminal coronal angioplasty
DSA	Digital subtraction angioplasty
H & E	stain Hematoxylin and eosin stain

References

1. Altes TA, Cloft HJ, Short JG, et al. 1999 ARRS Executive Council Award Creation of saccular aneurysms in the rabbit; a model suitable for testing endovascular devices. *Am J Roentgenol* 2000; 174: 349–354.
2. Krings T, Hans FJ, Moller-Hartmann W, et al. Treatment of experimentally induced aneurysms with stents. *Neurosurgery* 2005; 56: 1347–1360.
3. Nishi S, Nakayama Y, Ishibashi-Ueda H, et al. Occlusion of experimental aneurysms with heparin-loaded, microporous stent grafts. *Neurosurgery* 2003; 53: 1397–1405.
4. Nishi S, Nakayama Y, Ishibashi-Ueda H, et al. Development of microporous self-expanding stent grafts for treating cerebral aneurysms: designing micropores to control intimal hyperplasia. *J Artif Organs* 2011; 14: 348–356.
5. Geremia G, Brack T, Brennecke L, et al. Occlusion of experimentally created fusiform aneurysms with porous metallic stents. *AJNR Am J Neuroradiol* 2000; 21: 739–745.
6. Link J, Feyerabend B, Grabener M, et al. Dacron-covered stent-grafts for the percutaneous treatment of carotid aneurysms: effectiveness and biocompatibility-experimental study in swine. *Radiology* 1996; 200: 397–401.
7. Szikora I, Guterman LR, Wells KM, et al. Combined use of stents and coils to treat experimental wide-necked carotid aneurysms: preliminary results. *AJNR Am J Neuroradiol* 1994; 15: 1091–1102.
8. Sedat J, Chau Y, Mondot L, et al. Endovascular occlusion of intracranial wide-necked aneurysms with stenting (Neuroform) and coiling: mid-term and long-term results. *Neuroradiology* 2009; 51: 401–409.
9. Izar B, Rai A, Raghuram K, et al. Comparison of devices used for stent-assisted coiling of intracranial aneurysms. *PLoS One* 2011; 6: e24875.
10. Kim BM, Kim DJ and Kim DI. Stent application for the treatment of cerebral aneurysms. *Neurointervention* 2011; 6: 53–70.
11. Flugelman MY, Virmani R, Leon MB, et al. Genetically engineered endothelial cells remain adherent and viable after stent deployment and exposure to flow in vitro. *Circ Res* 1992; 70: 348–354.
12. Nishi S, Nakayama Y, Ueda H, et al. A new stent graft with thin walled controlled micropored polymer covering. *Intervent Neuroradiol* 2000; 6(Suppl 1): 175–180.
13. Hue L and Greisler HP. Biomaterials in the development and future of vascular grafts. *J Vasc Surg* 2003; 37: 472–480.
14. Farrar DJ, Litwak P, Lawson JH, et al. In vivo evaluations of a new thrombo-resistant polyurethane for artificial heart blood pumps. *J Thorac Cardiovasc Surg* 1988; 95: 191–200.
15. Giancario M, Mirko DO, Lacono C, et al. Gastrointestinal artery stamp hemorrhage following pylorus-sparing whipple procedure: treatment with covered stents. *Dig Surg* 2002; 19: 237–240.
16. Kikumoto R, Tamao Y, Tezuka T, et al. Selective inhibition of thrombin by (2R, 4R)-4-methyl-1-(N2-(3-methyl-1,2,3,4-tetra-hydro-8quinolinyl)   sulfonyl)-1-arginyl))-2-piperidinecarboxylic acid. *Biochemistry* 1984; 23: 85–90.
17. Kumada T and Abiko Y. Comparative study on heparin and a synthetic thrombin inhibitor no. 805 (MD-805*) in experimental antithrombin 3-deficient animals. *Thromb Res* 1981; 24: 285–298.
18. Imanishi T, Arita M, Hamada M, et al. Effects of locally administration of argatroban using a hydrogel-coated balloon catheter on intimal thickening induced by balloon injury. *Jpn Circ J* 1997; 61: 256–262.

19. Richey T, Iwata H, Oowaki H, et al. Surface modification of polyurethane balloon catheters for local drug delivery. *Biomaterials* 2000; 21: 1057–1065.

20. Miskolczi L, Guterman LR, Flaherty JD, et al. Saccular aneurysm induction by elastase digestion of the arterial wall: a new animal model. *Neurosurgery* 1998; 43: 595–600.

21. Kallmes DF, Helm GA, Hudson SB, et al. Histologic evaluation of platinum coil embolization in an aneurysm model in rabbits. *Radiology* 1999; 213: 217–222.

22. Lopes DK, Ringer AJ, Boulus AS, et al. Fate of branch arteries after intracranial stenting. *Neurosurgery* 2008; 52: 1275–1279.

23. Wakhloo AK, Tio FO, Lieber BB, et al. Self-expanding nitinol stents in canine vertebral arteries; Hemodynamics and tissue response. *AJNR Am J Neuroradiol* 1995; 16: 1043–1051.

24. Wakhloo AK, Schellhammer P, de Vries J, et al. Self-expanding and balloon-expandable stents in the treatment of carotid aneurysms: an experimental study in a canine model. *AJNR Am J Neuroradiol* 1994; 15: 493–502.

25. Saatci I, Yavuz K, Ozer C, et al. Treatment of intracranial aneurysms using the pipeline flow-diverter embolization device: a single-center experience with long-term follow-up results. *AJNR Am J Neuroradiol* 2012; 33: 1436–1446.

288

In-body tissue-engineered aortic valve (Biovalve type VII) architecture based on 3D printer molding

Yasuhide Nakayama,[1] Yoshiaki Takewa,[2] Hirohito Sumikura,[2] Masashi Yamanami,[1,3]
Yuichi Matsui,[1,4] Tomonori Oie,[1] Yuichiro Kishimoto,[2] Mamoru Arakawa,[2] Kentaro Ohmuma,[2]
Tsutomu Tajikawa,[4] Keiichi Kanda,[3] Eisuke Tatsumi[2]

[1]Division of Medical Engineering and Materials, National Cerebral and Cardiovascular Center Research Institute, Osaka, Japan
[2]Department of Artificial Organs, National Cerebral and Cardiovascular Center Research Institute, Osaka, Japan
[3]Department of Cardiovascular Surgery, Kyoto Prefectural University of Medicine, Kyoto, Japan
[4]Department of Mechanical and Systems Engineering, Kansai University, Osaka, Japan

Abstract: In-body tissue architecture—a novel and practical regeneration medicine technology—can be used to prepare a completely autologous heart valve, based on the shape of a mold. In this study, a three-dimensional (3D) printer was used to produce the molds. A 3D printer can easily reproduce the 3D-shape and size of native heart valves within several processing hours. For a tri-leaflet, valved conduit with a sinus of Valsalva (Biovalve type VII), the mold was assembled using two conduit parts and three sinus parts produced by the 3D printer. Biovalves were generated from completely autologous connective tissue, containing collagen and fibroblasts, within 2 months following the subcutaneous embedding of the molds (success rate, 27/30). In vitro evaluation, using a pulsatile circulation circuit, showed excellent valvular function with a durability of at least 10 days. Interposed between two expanded polytetrafluoroethylene grafts, the Biovalves ($N = 3$) were implanted in goats through an apico-aortic bypass procedure. Postoperative echocardiography showed smooth movement of the leaflets with minimal regurgitation under systemic circulation. After 1 month of implantation, smooth white leaflets were observed with minimal thrombus formation. Functional, autologous, 3D-shaped heart valves with clinical application potential were formed following in-body embedding of specially designed molds that were created within several hours by 3D printer. © 2014 Wiley Periodicals, Inc. J Biomed Mater Res Part B: Appl Biomater 00B:000–000, 2014.

Key Words: tissue engineering, heart valve, 3D printer, connective tissue, surgery

INTRODUCTION

Surgical alternatives for end-stage valvular heart disease consist of the application of either mechanical or biological prostheses, both of which have significant limitations.[1] Although mechanical valves have a functional life span of at least 25 years, they are associated with the need for life-long anticoagulation and the concomitant risks of thromboembolism and bleeding. Biological prostheses, generally, have better hemodynamic characteristics and do not require long-term anticoagulation, but are associated with progressive tissue deterioration. Therefore, tissue-engineering techniques may play a prominent role in the future development of heart valve replacements. Much of the research designed to create in vitro tissue-engineered heart valves has focused on the scaffold materials, culturing of cells, and the use of appropriate seeding and preconditioning protocols.[2,3] However, the mechanical integrity of the replacement valves and their abil-

ity to withstand systemic pressures depends on the neotissue. Therefore, the clinical utility of these autologous tissue-engineered heart valves is limited, particularly in growing children.

The medical and engineering relevance of computer-based three-dimensional (3D) procedures—known as 3D printing—is increasing, which increases the potential of rapid prototyping techniques.[4,5] The technology presented in this paper is based on the principle of building 3D models, layer by layer, and enables the direct manufacturing of precise, complex-shaped implants using biocompatible or biodegradable materials from computerized data in several medical areas.[6–9]

As a feasible, regenerative medicine approach, we developed completely autologous valved conduits, named Biovalves,[10–12] without any artificial scaffolds, through the use of "in-body tissue architecture" technology. This autologous

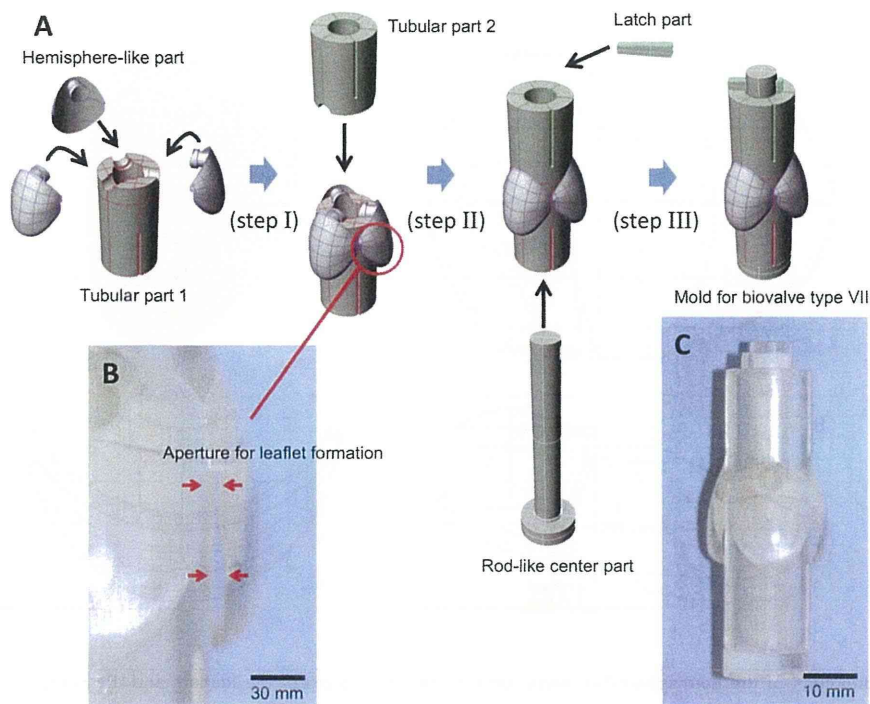Correspondence to: Y. Nakayama (e-mail: ny@ncvc.go.jp)

1

FIGURE 1. (A) Schematic diagram of the assembly process of seven parts (three hemisphere-like parts, two tubular parts, rod-like center part and latch part) for the mold in three steps. (B) Photo of the aperture (between red arrows) for leaflet formation. (C) Photo of the assembled mold. [Color figure can be viewed in the online issue, which is available at wileyonlinelibrary.com.]

method is based on the phenomenon of tissue encapsulation of foreign materials implanted in living bodies.[13] The technology offers the following advantages: the developed tissue prostheses are non-toxic, particularly non-carcinogenic, and can be fabricated in a wide range of shapes and sizes to suit the needs of individual recipients. In addition, the prostheses, without any artificial materials, possess the characteristics of their natural counterparts, including anticoagulation, self-repair, tissue regeneration, and growth adaptability. These prostheses do not require complex *in vitro* cell management procedures or exceptionally clean laboratory facilities, both of which are expensive and labor-intensive over long periods.

In an early development stage, Biovalves were prepared in small size animal models such as rats or beagle dogs, which are less relevant for heart valve testing. In the present paper, we used a 3D printer to produce a Biovalve mold. The clinical feasibility of the Biovalves obtained from the mold was evaluated by implanting the aortic Biovalve in a big size animal using a goat model for estimation of aortic valuvalar performance in a human systemic circulation condition, after evaluating their function and durability *in vitro*.

MATERIALS AND METHODS
Animal studies
The animal studies were performed in accordance with the "Guide for the Care and Use of Laboratory Animals," published by the United States National Institutes of Health (NIH Publication No. 85-23, revised 1996) under a protocol approved by the National (Japan) Cerebral and Cardiovascular Center Research Institute Committee (No. 12002).

Mold preparation
Seven fine plastic parts [Figure 1(A)], produced using a 3D digital printer (Projet HD3000, 3D Systems, Rock Hill, SC), were assembled to create the molds [Figure 1(C)]. First, three small hemispherical parts (Figure 2) for the sinus of the Valsalva were fastened between the two tubular parts of the conduit (diameter, 16 mm), with a small, 1-mm aperture between the three hemispherical parts and the tubular part [steps I and II in Figure 1(A)]. Second, the combined parts (height, 5 cm) were fixed with a central rod and a latch to obtain the final mold (step III). The mold was based on the geometry of a goat aortic valve and was designed for the formation of the leaflets that are separated from each other in the open position.

Biovalve preparation
A total of 30 molds were placed into dorsal subcutaneous pouches in 10 goats (age, 1–2 years; body weight, 40–50 kg), under general anesthesia induced with 10 mg/kg of ketamine and maintained with 1–3% isoflurane. The leaflet formation at the three apertures was non-invasively observed using a capsule endoscope[14] (EC Type 1, Olympus, Tokyo, Japan), present in one of the tubular parts of the mold [Figure 3(A)]. Two months later, after complete encapsulation with connective tissue, the structures were harvested [Figure 3(B)]. Biovalves, with three protrusions resembling the sinuses of Valsalva [Figure 3(E)], were obtained by removing all of the parts from the ends of the developed tubular tissue. The three membranous leaflets had formed in the open position inside the conduit. Each leaflet had an area of 2.4 cm^2, with a height
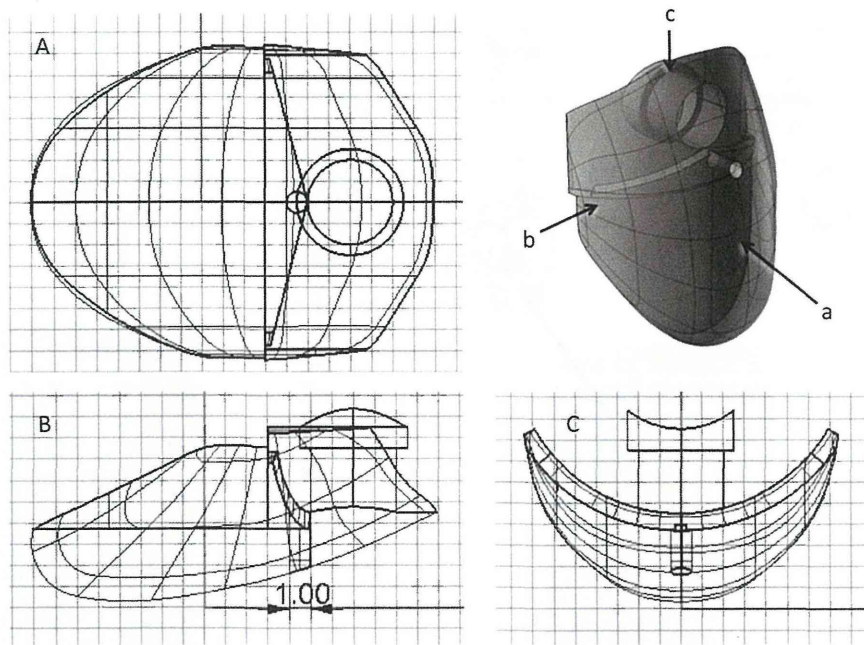
FIGURE 2. Projection drawings of the hemisphere-like parts used in the preparation of the leaflets and the sinus of Valsalva (A, front view; B, side view; C, top view).
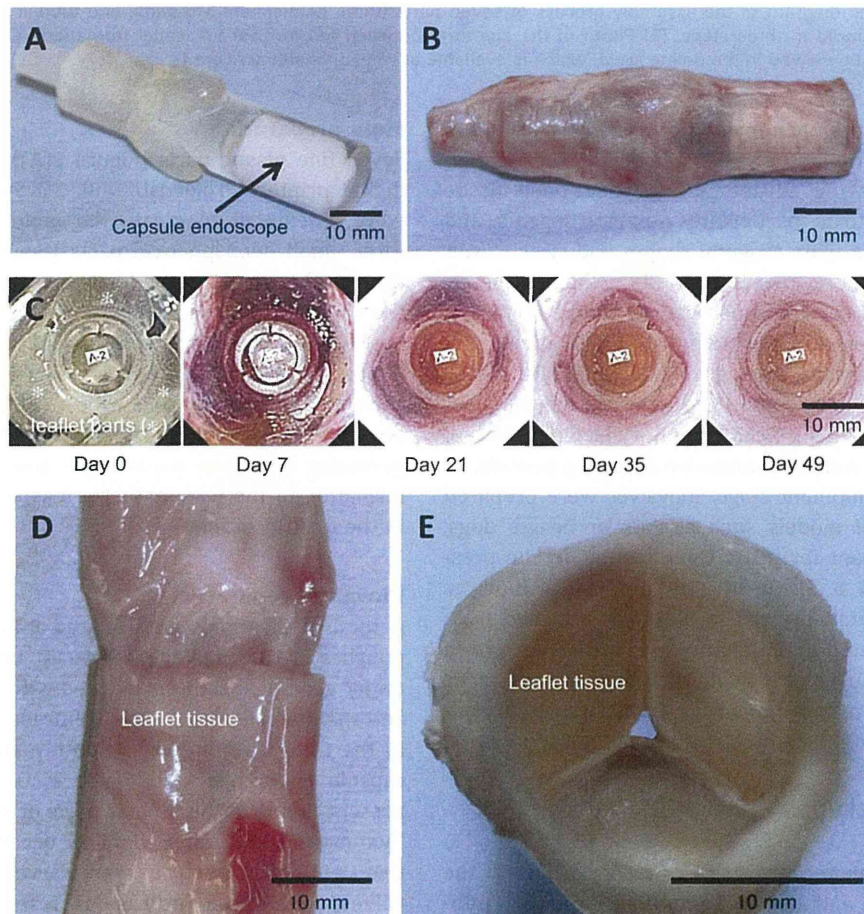

FIGURE 3. Photos of the preparation mold, impregnated with a capsule endoscope, (A) before and (B) after encapsulation. (C) The leaflet formation process at the aperture of the mold observed using a capsule endoscope non-invasively. Photos of (D) the luminal surface of the Biovalve and (E) the closed form with three protrusions resembling the sinus of Valsalva. [Color figure can be viewed in the online issue, which is available at wileyonlinelibrary.com.]
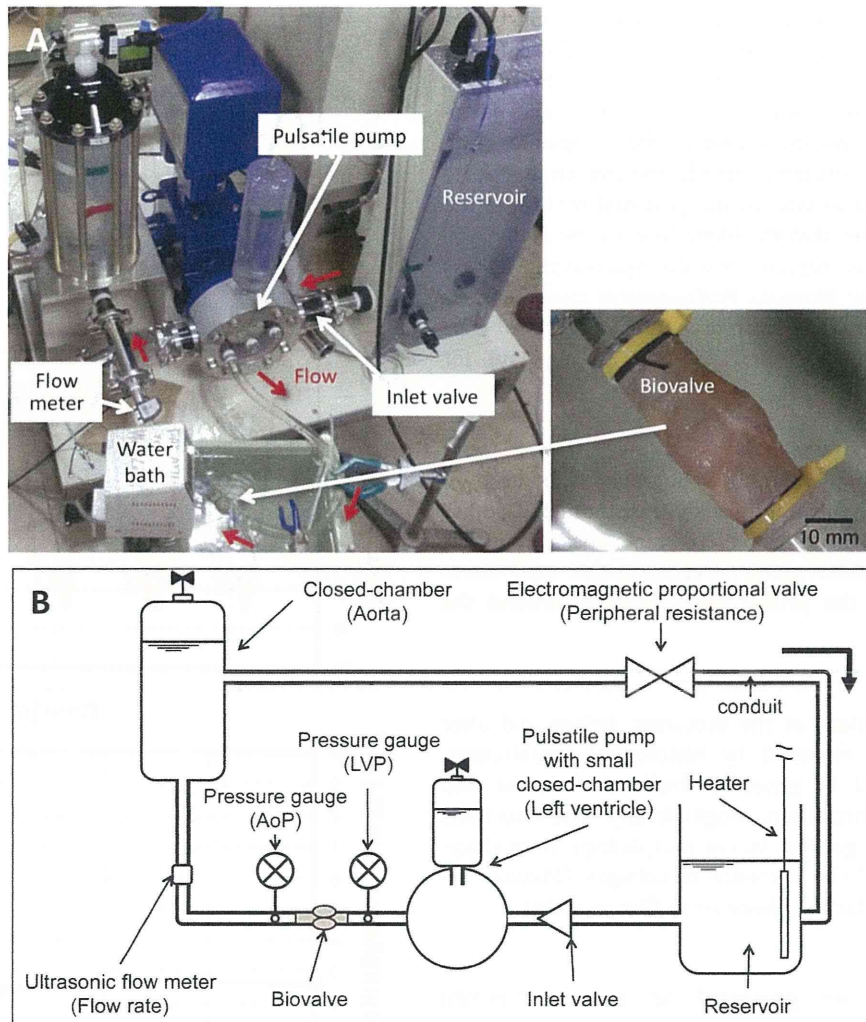
FIGURE 4. (A) Photo and (B) schematic diagram of the pulsatile circulation circuit connected with the Biovalve in a 37°C water bath. [Color figure can be viewed in the online issue, which is available at wileyonlinelibrary.com.]

of 1.7 cm. Of the 27 successfully constructed Biovalves, we randomly selected five for *in vitro* evaluations of their valve functions, five for elastic modulus measurements, and three for transplantation into the goat model.

Elastic modulus

The tensile strengths of the Biovalve tissues were measured using a uniaxial tensile-testing apparatus (Rheoner II, Yama-den, Tokyo, Japan). Each sample was cut into rectangular strips (5-mm wide) and fixed to the upper and lower grips (initial length, 5 mm). A tensile load was applied by moving the lower grip at a rate of 0.05 mm/s until failure, that is, tissue rupture. The maximum elastic modulus before rupture was obtained from the slope of the stress–strain curve.

In vitro functionality tests

Biovalves were connected to a pulsatile circulation circuit (LaboHeart NCVC, IWAKI, Tokyo, Japan; Figure 4). The valvular functions of the Biovalves were examined at 37°C, under pulsatile conditions designed to simulate human systemic circulation (pressure, 49–129 mmHg; beat rate, 70–

120 beats/min). The mean regurgitation was calculated from 10 beat cycles. The degree of regurgitation (Re) was defined according to the following equation.

Re (%) = amount of the reverse flow/amount of the forward flow × 100

Biovalve implantation

Biovalves were implanted into the previously used goats (*N* = 3), which were premedicated with ketamine (10 mg/kg), intubated, and anesthetized with isoflurane (1–3%). Each animal's heart was exposed through a left thoracotomy at the fifth subcostal region. Both ends of the Biovalve conduit were anastomosed to expanded polytetrafluoroethylene (ePTFE) grafts (internal diameter, 14 mm × 20 cm; GORE-TEX, W. L. Gore & Associates, Newark, DE).

After systemic heparinization (200 U/kg), the distal end of each composite graft was anastomosed to the descending aorta in an end-to-side manner under a partially occluding clamp. A felt cuff was sewn to the left ventricular apex. The apex was cored with a 19-mm, custom-made, ventricular coring device. Thereafter, an apical-left ventricle connector,

composed of a custom-made, stainless steel conduit and a 14-mm ePTFE graft, were inserted through the felt cuff into the apex and tied to the felt cuff. To complete the bypass, the grafted part of the connector was sewn, in an end-to-end manner, to the proximal end of the composite graft, thus interposing the Biovalve. Finally, the descending aorta was ligated, with vessel tape, at the proximal portion of the anastomosis to ensure that the blood flow to the abdominal aorta was completely supplied via the apico-aortic bypass that incorporated the Biovalve. Postoperative systemic anti-coagulation was maintained with oral administration of warfarin sodium (3 mg/day) and aspirin (81 mg/day) for 1 month.

In vivo functionality tests

Immediately after implantation, angiography was used to evaluate the valvular function; weekly transthoracic Doppler echocardiography was utilized thereafter. Bypass flow was continuously monitored using electromagnetic and ultrasonic flow meters; the probes were attached around the ePTFE grafts.

Tissue analyses

The tissue compositions of the Biovalves, before and after implantation, were assessed by histological examination. Samples were fixed in phosphate-buffered formalin and embedded in paraffin; 5-μm, longitudinally sliced sections were examined for general tissue morphology (hematoxylin–eosin stain) and the presence of collagen (Masson trichrome stain) and elastin (Elastica-van Gieson stain).

Statistics

Quantitative data are presented as means ± standard deviation.

RESULTS

Preparation of biovalves

Figure 1 shows schematic diagram of the assembly process of the fine plastic mold parts. All parts, including the complex-shaped hemispherical components (Figure 2), were precisely produced by 3D printer within several hours [Figure 1(A)]. The hemispherical parts were used for the formation of the leaflets and the sinus of Valsalva. These were placed on a tubular section prepared by connecting the two rod-like parts [steps I and II in Figure 1(A)] with a small aperture for leaflet formation [Figure 1(B)]. The combined components were fixed with a rod-like part and a latch [step III in Figure 1(A)]. The resultant molds [Figure 1(C)] were completely encapsulated with autologous connective tissues during the preparation process [Figure 3(B)]. The molds, impregnated in the developed tissue, were easily removed by separating the assembled parts without any resultant tissue damage. Thin membranous tissues developed at the three apertures between the tubular part and the three hemispherical parts, forming three leaflets inside the conduit tissue [Figure 3(D)]. When the leaflet tissues were blown, a closed Biovalve was obtained [Figure 3(E)].
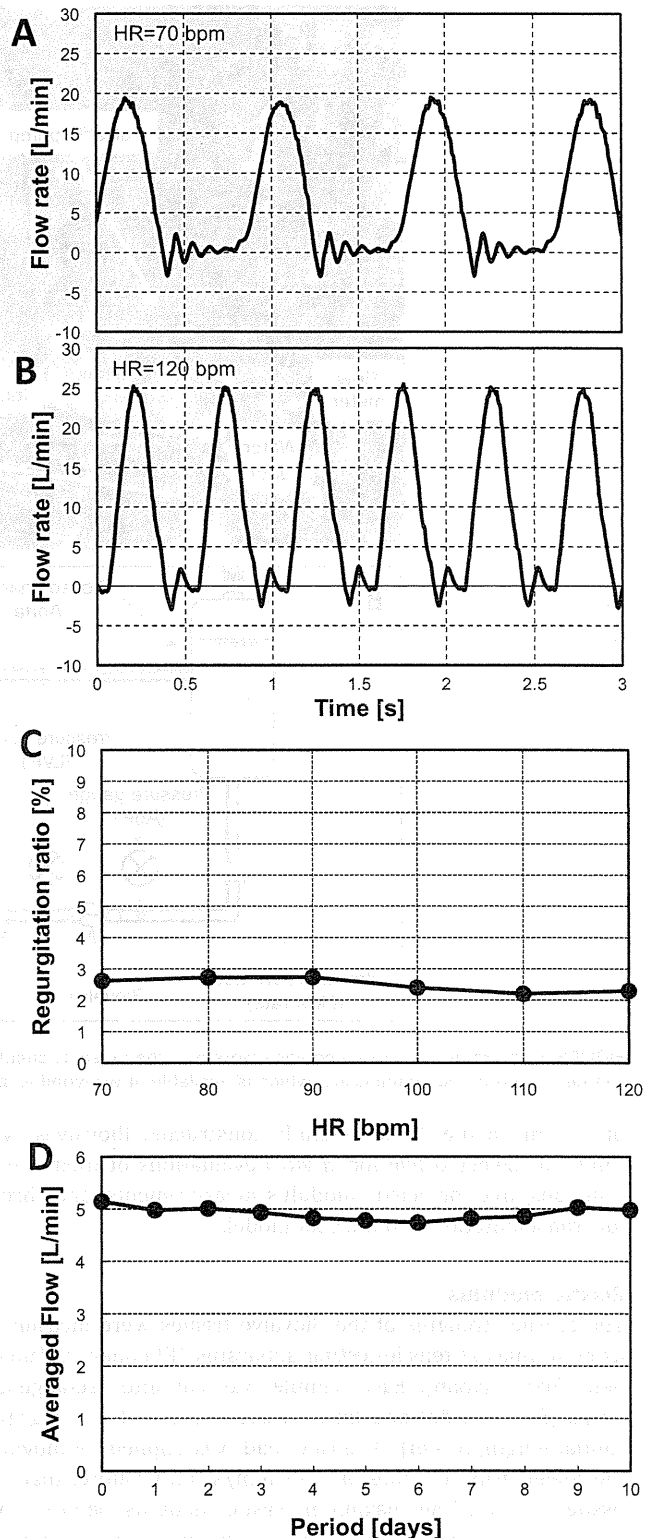

FIGURE 5. Pulsatile flow waveforms of Biovalves with a pulsatile flow rate of (A) 70 beats/min and (B) 120 beats/min. (C) Regurgitation ratio change under different heart rate from 70 to 120 bpm. (D) Averaged flow change up to 10 days.

Observation of the leaflet formation, using a capsule endoscope [Figure 3(A)], revealed that tissue ingrowth into the apertures occurred gradually, with concurrent capillary
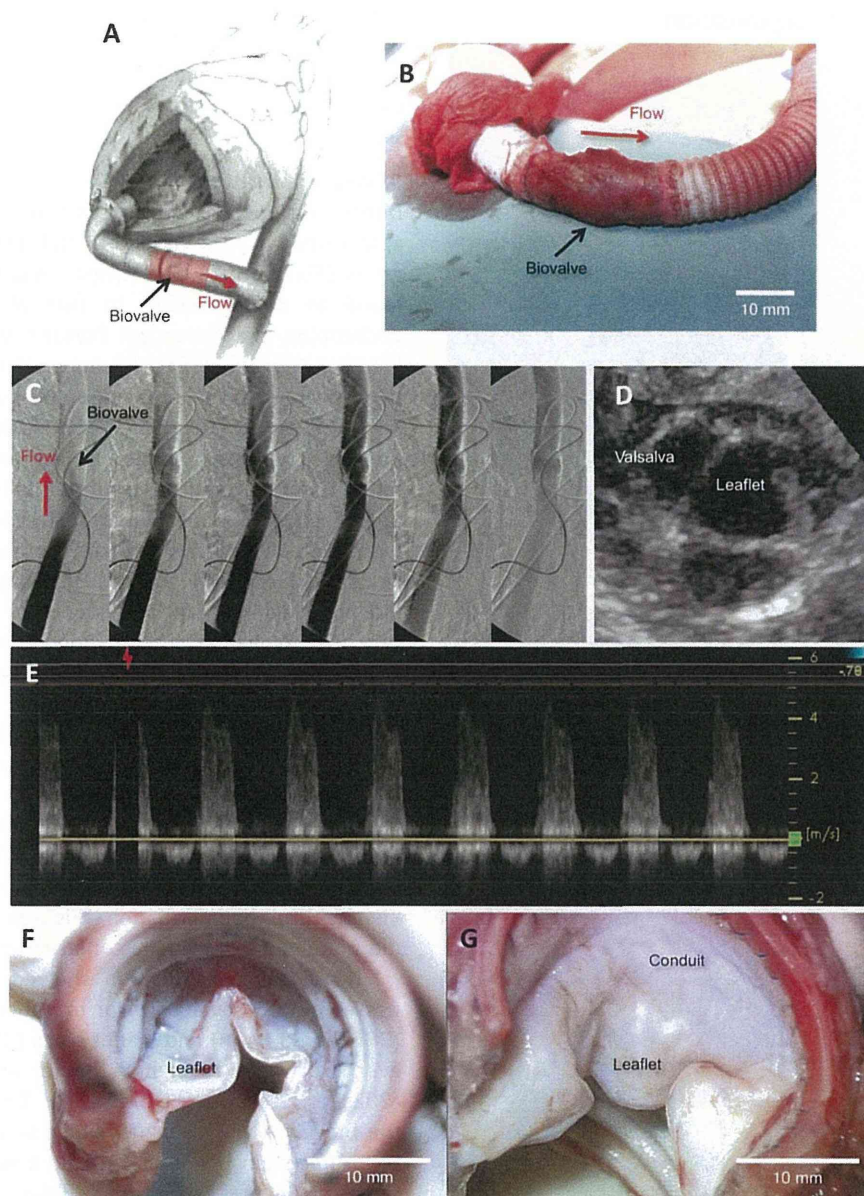
FIGURE 6. (A) Schematic picture of the implantation model via an apico-aortic bypass method. (B) Photo of the Biovalve implanted by interposing between artificial garfts. (C) Intraoperative angiography immediately after implantation. Leaflet observation at circumferential section (D) and flow measurement (E) by transthoracic doppler echocardiography. Macroscopic photos of Biovalves after 1 month of implantation: views from the aortic side (F) and the ventricular side (G). [Color figure can be viewed in the online issue, which is available at wileyonlinelibrary.com.]

formation [Figure 3(C)]. After being implanted for 49 days, the apertures were completely replaced by autologous connective tissues to form leaflet tissues in the molds. The success rate of Biovalve preparation using this method was 90% (27/30). In two molds collapse of the hemispherical parts in the molds occurred, possibly due to the lack of strength of the mold material. In 1 mold, inflammation was observed due to infection. The 27 usable Biovalves had well-formed, tubular-shapes, with three protrusions resembling the sinus of Valsalva; the quality of the Biovalves appeared to be almost identical [Figure 3(E)]. Inside the conduit, three separate membranous leaflets were present and were connected at the commissure without an aperture.

The maximum elastic modulus of the leaflet part of Biovalves was 1083 ± 288 kPa, which was very close to that of a natural goat leaflet (1097 ± 389 kPa). The conduit part of each Biovalve was significantly more robust (2800 ± 610 kPa)—approximately six-times that of the goat aorta (494 ± 169 kPa).

In vitro valve function

Valvular functioning of Biovalves was examined using a pulsatile circuit (Figure 4). Figures 5A, B indicate the typical flow waveforms, compared at 70 and 120 beats/min, respectively, with a mean flow rate of 5.0 L/min and an aortic pressure of 129–49 (mean, 82.2) mmHg. For all
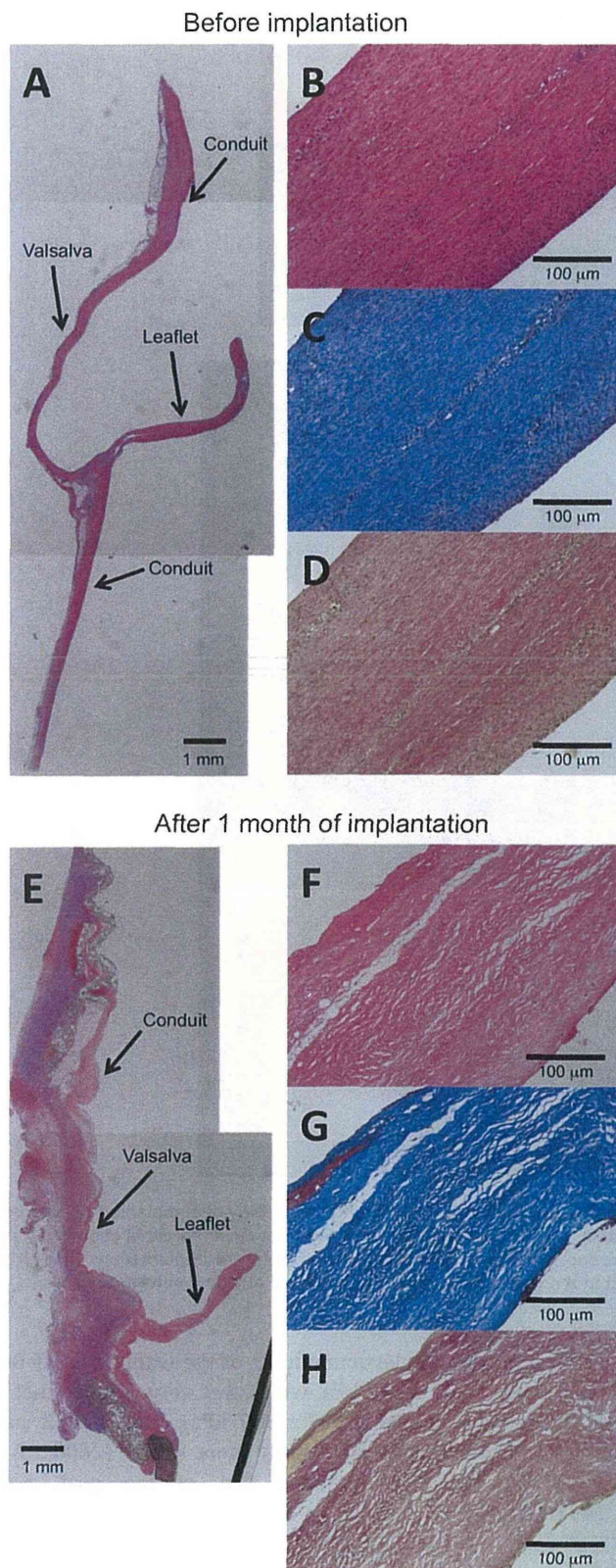
FIGURE 7. Tissue morphology of Biovalves (A–D) before and (E–H) after 1 month of implatation. A, B, E, and F; hematoxylin and eosin staining, C and G; Masson's trichrome stain; D and H; Elastica-van Gieson stain. The upper portion is the distal side and the lower portion is the proximal side in all the images. [Color figure can be viewed in the online issue, which is available at wileyonlinelibrary.com.]

Biovalves ($N = 5$), regurgitation during the diastolic phase was <3% [Figure 5(C)]. In addition, the mean flow rate (4.9 L/min) was maintained for at least for 10 days in a saline solution at 37°C [Figure 5(D)].

In vivo application

During interposed implantation of the Biovalve into an apico-aortic bypass via end-to-end anastomosis with ePTFE grafts [Figure 6(A)], the surgical handling of Biovalves was found to be equivalent to that of native tissues. After declamping, the connected Biovalve pulsated with minimal bleeding [Figure 6(B)]. Intraoperative angiography of the bypass circuit after implantation, revealed protrusions, similar to those of the sinus of Valsalva, with leaflets that opened and closed smoothly; moreover, there was good blood flow and minimal regurgitation [Figure 6(C)]. Up to 1 month after implantation, transthoracic echocardiographic examinations revealed protrusions similar to those of the sinus of Valsalva [Figure 6(D)]. Doppler echocardiography did not yield substantial evidence of stenosis or regurgitation. The Biovalves showed good forward flow during the systolic phase and trivial regurgitation during the diastolic phase [Figure 6(E)]. Bypass flow was maintained at 2.6 ± 1.1 L/min throughout the implantation period.

The protrusions resembling those of the sinus of Valsalva did not significantly change in size or shape within the 1-month period after implantation [Figure 6(F)]. All blood contact surfaces, including the luminal surface of the conduit and leaflet surfaces, were white and had minimal visible thrombus formation [Figures 6(F, G)]. The leaflets did not show any evidence of structural damage.

Histological examination showed consistent wall thicknesses in the Biovalves, prior to implantation, at the conduit (287.5 ± 33.1 μm) and leaflet parts (350.0 ± 58.0 μm); however, the wall was slightly thinner at the sinus of Valsalva (202.5 ± 31.1 μm) [Figure 7(A)]. The main component of the Biovalves was collagen, which stains blue with Masson's trichrome stain [Figure 7(E)], and a minimal amount of elastic fiber [Figure 7(D)]; the cellular components were also minimal [Figure 7(B)]. Both surfaces of the leaflets were very smooth.

After implantation, the wall thickness of the leaflet membrane was generally well maintained (332.3 ± 82.5 μm), whereas the thickness at the sinus of Valsalva decreased (<100 μm); however, at the sinus of Valsalva, there was a thick lining of connective tissue that had migrated from the surrounding tissue [Figure 7(E)]. The remaining tissues consisted of extracellular matrix, which remained predominantly collagenous [Figures 7(G, H)]. Minimal cell ingrowth was evident [Figure 7(F)].

DISCUSSION

The technology used in this report required several months to produce the tissue prostheses. However, a management process, including cell incubation, was not required for during the tissue formation period. The implantable, autologous tissues were naturally formed according to the shape of the

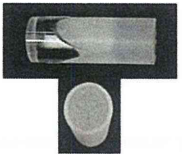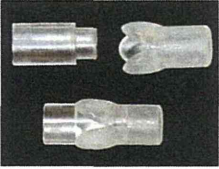**TABLE I. Comparison of Several Types of Biovalves**
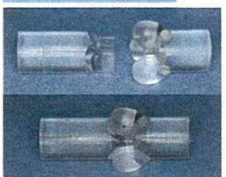
Type	Mold and Its Materials		Embedding Into	Biovalve and Its Composition		Implantation Into	Characteristics and Problems	References
I		SI rod covered with PU sponge crown	Rabbit		AT crown-shaped PU	na	Aortic valve replacement type. Mechanical properties of Biovalve leaflets were statistically equivalent to those of porcine ones. PU was remained in Biovalve.	11
II		Assembly of concave SI rod and convex AC rods (upper), covered with PU sponge tube (lower)	Rabbit		AT PU tube	na	Conduit type. PU was remained in Biovalve.	18
III		AT connective tissue-covered SI rod partially rapped with PU tubular sheet	Rabbit		AT	na	Conduit type by completely autologous tissue without any artificial material. Two-times in-body tissue architecture process was needed.	19
IV		Assembly of concave and convex SI rods (upper), covered with PU mesh tube (lower)	Rabbit		AT Tubular PU mesh	na	Conduit type with the sinus of Valsalva. PU was remained in Biovalve.	20
V		Concave and convex-shaped SI rods (upper) and their assembly (lower)	Beagle dog		AT	Beagle dogs as a pulmonary valve (84 days)	Completely autologous conduit type tissue with the sinus of Valsalva. The three commissures had large aperture depending on the mold design. Before implantation suturing of the apertures was needed to avoid regurgitation.	10

TABLE I. Continued

Type	Mold and Its Materials	Embedding Into	Biovalve and Its Composition		Implantation Into	Characteristics and Problems	References
VI		Concave AC rod by 3D printer and convex SI rod (upper), and their assembly (lower)	Goat		AT	Goats as an aortic valve (2 months)	Completely autologous conduit type tissue with the sinus of valsalva. Low regurgitation rate (12.7%) and high opening ratio (ca. 50%) by leaflet formation at its open position. The size of Valsalva was limited to low to avoid tissue damage at mold removing process.	12 and 21
VII		Assembly of AC parts by 3D printer (upper) and with capsule endoscope (lower)	Goat		AT	Goats as an aortic valve (1 month)	Completely autologous conduit type tissue with the sinus of valsalva similar to native shape and size. Extremely low regurgitation rate (<3%). The mold parts could be removed by step-by-step separation from the formed Biovalve without any tissue damage.	22

Abbreviations: SI, silicone; PU, polyurethane; AC, acrylate; AT, autologous tissue.